REVIEW

From the intrinsic properties to the functional role of a neuron phenotype: an example from electric fish during signal trade-off

Javier Nogueira[1,2] and Angel A. Caputi[2,*]

[1]Departamento de Histología y Embriología, Facultad de Medicina, Universidad de la República, Avenida General Flores, 2125 Montevideo, Uruguay and [2]Departamento de Neurociencias Integrativas y Computacionales, Instituto de Investigaciones Biológicas Clemente Estable, Avenida Italia, 3318 Montevideo, Uruguay

*Author for correspondence (caputiangel@gmail.com)

Summary

This review deals with the question: what is the relationship between the properties of a neuron and the role that the neuron plays within a given neural circuit? Answering this kind of question requires collecting evidence from multiple neuron phenotypes and comparing the role of each type in circuits that perform well-defined computational tasks. The focus here is on the spherical neurons in the electrosensory lobe of the electric fish *Gymnotus omarorum.* They belong to the one-spike-onset phenotype expressed at the early stages of signal processing in various sensory modalities and diverse taxa. First, we refer to the one-spike neuron intrinsic properties, their foundation on a low-threshold K$^+$ conductance, and the potential roles of this phenotype in different circuits within a comparative framework. Second, we present a brief description of the active electric sense of weakly electric fish and the particularities of spherical one-spike-onset neurons in the electrosensory lobe of *G. omarorum*. Third, we introduce one of the specific tasks in which these neurons are involved: the trade-off between self- and allo-generated signals. Fourth, we discuss recent evidence indicating a still-undescribed role for the one-spike phenotype. This role deals with the blockage of the pathway after being activated by the self-generated electric organ discharge and how this blockage favors self-generated electrosensory information in the context of allo-generated interference. Based on comparative analysis we conclude that one-spike-onset neurons may play several functional roles in animal sensory behavior. There are specific adaptations of the neuron's 'response function' to the circuit and task. Conversely, the way in which a task is accomplished depends on the intrinsic properties of the neurons involved. In short, the role of a neuron within a circuit depends on the neuron and its functional context.

Key words: self-generated signal, allo-generated signal, intrinsic properties, fast electrosensory pathway, one-spike-onset neuron.

Received 8 November 2012; Accepted 10 April 2013

Introduction

This review deals with a relatively unexplored, poorly understood, but fundamental question in integrative neuroscience: what is the relationship between the properties of a neuron and the role that a neuron plays within a given neural circuit? (Ramón y Cajal, 1899; Llinás, 1988; Arbib et al., 1998; Migliore and Shepherd, 2005; Marder, 2011). From the work of Ramón y Cajal (Ramón y Cajal, 1899), who implicitly introduces this problem by stating the rules of dynamic polarity and economy, many advances have been made in describing circuit wirings, and the properties of the neurons and the synapses that connect them. Further work by Llinás led to the 'law of non-interchangeability' of neurons (Llinás, 2001). This hypothesis suggests that the function of a circuit depends not only on synaptic connections and the types of neurotransmitter involved, but also on the dynamic properties of neurons. The other aspect of this assertion is that for specific tasks in specific circuits, nature evolved specific neuron phenotypes. Each neuron is characterized by its morphology, ion channel repertoire and subcellular distribution, and intracellular system of second messengers. The specific combination of such features provides the neuron with a phenotypic identity that can be characterized as the 'neuron's response function', which determines the firing pattern under a given arrangement of synaptic inputs or stimuli (Izhikevich, 2006). According to this view, Migliore and Shepherd proposed the concept of neuronal 'functional phenotypes' as a way of combining intrinsic properties, morphology and emerging functional properties (Migliore and Shepherd, 2005).

Nonetheless, the role of a neuron within a circuit depends on two factors: the neuron and its functional context. From a bottom-up view, one can only predict potential neuron roles depending on their connectivity, characteristics, and location of the synapses and their intrinsic properties. The exclusive use of a bottom-up approach is not enough because: (1) different combinations of basic structural characteristics may result in an identical functional phenotype expressed by different neurons; (2) the same neuron phenotype may play different roles in different circuits; and (3) there are multiple solutions for producing similar circuit performance.

From a top-down view, one must characterize the task, the neuro-computational algorithms and determine which properties of the neuron may be necessary, or at least appropriated for implementing such an algorithm (Marr, 1982).

Neither top-down nor bottom-up approaches alone are sufficient for understanding a neuron's role in a circuit (Churchland et al., 1990). Its potential is only is expressed when the neuron plays its role during a behavioral task (Wagner and Gaese, 2005). While the 'response function' sets the potential derived from the structural properties of a neuron (Arbib et al., 1998), the function of a neuron is the actual role that a neuron phenotype plays in a task performed
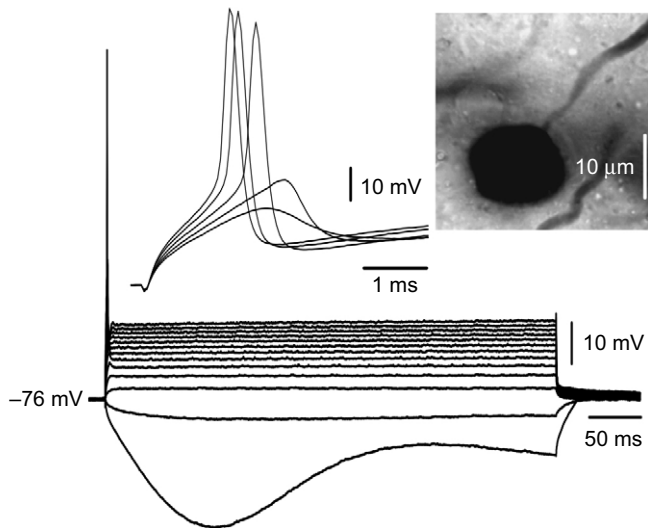
Fig. 1. Spherical cell phenotype. Responses to current steps. The spherical cells bear round smooth somatas ~15 μm in diameter and thick axons with a thin initial segment (a retrogradely marked neuron is shown in the right inset). Current steps depolarizing the cell between –65 and −40 mV elicited an early graded 'hump', peaking between 1.9 and 2.6 ms after the pulse onset. With depolarizations larger than −40 mV, a single spike at the pulse onset is evoked independently of the stimulus intensity. After the hump or the spike, the membrane potential remained clamped at a constant value, increasing linearly with the stimulus amplitude. Hyperpolarizing steps of the same absolute intensity systematically caused a larger departure from the resting potential. After 20–70 ms, hyperpolarization was followed by a depolarizing sag. The left inset shows a few traces at a different magnification. Note the hump and the decrease in spike latency with increasing stimulus intensity.

by a given circuit. A Spanish philosopher wrote 'yo, soy yo y mi circunstancia' (Ortega y Gasset, 1914). Paraphrasing, we propose that 'a neuron is the neuron phenotype and its anatomo-functional context', meaning that a neuron phenotype would be functionally expressed only when it is integrated in a neural network and under a functional context. Therefore, to understand a neuronal circuit it is important to measure both the network behavior and the properties of several of its components, and to look for correlations between them and with the performance of the circuit and/or animal (Marder, 2011).

Weakly electric fish have been a good model for understanding relationships between neurons and behavior (Fessard, 1974; Bullock and Heiligenberg, 1986; Kramer, 1990; Heiligenberg, 1977; Heiligenberg, 1991; Moller, 1995; Bullock et al., 2005). Here we deal with this problem in the specific case of spherical neurons of the electrosensory lobe of the electric fish *Gymnotus omarorum* (Richer-de-Forges et al., 2009). These are second-order neurons (Réthelyi and Szabo, 1973; Maler, 1979; Berman and Maler, 1999) inserted in a well-defined and simple circuit [the fast electrosensory pathway (Szabo et al., 1975)], whose activity can be experimentally studied in naturalistic conditions (Castelló et al., 1998) during well-defined behavioral patterns such as 'jamming avoidance' (Westby, 1974; Westby, 1979; Westby, 1981; Baker, 1980; Capurro et al., 1998; Capurro et al., 1999; Lorenzo and Macadar, 2005) and 'synchronization bouts' (Westby, 1974).

The phenotype: the one-spike-onset neurons

These cells respond with a single spike at the beginning of a current step injection independent of the amplitude of the injected current.

At the end of positive current injections, onset neurons show a prominent after-hyperpolarization (Fig. 1). Additionally, one-spike-onset neurons develop a fast depolarizing sag during injection of negative current pulses and a rebound depolarization on termination of the negative current injection. These neurons typically show low noise and a stable resting membrane potential of approximately −70 mV.

One-spike cells are a convergent solution in the evolution of time-coding sensory systems, although species variations may adapt cell structure (including channel repertoire and distribution, geometry and internal signaling pathways) to specific functions. This cell phenotype is characteristic of the fast auditory pathways of higher vertebrates, occurring at different processing stages from the cochlear nuclei to the superior coliculi (Bal and Oertel, 2001; Manis and Marx, 1991; Carr, 1993; Koch and Grothe, 2003). They were also reported at the spinal ganglia (Yan et al., 2007) and dorsal horn of mammals (Prescott and De Koninck, 2002) and in the fast electrosensory pathways of gymnotiforms (Nogueira et al., 2006; Matsushita et al., 2012).

The intrinsic properties of one-spike-onset neurons are dominated by two resonant currents clamping the membrane potential at a stable level by negative feedback mechanisms. There is a persistent outward rectification dependent on a low-threshold K$^+$ conductance (K$^+_{LT}$), and an inward rectification mediated by a mixed-cation conductance (I_h) (Wu and Oertel, 1984; Manis and Marx, 1991; Reyes et al., 1994; Brew and Forsythe, 1995; Rathouz and Trussell, 1998; Trussell, 1999; Golding et al., 1999; Oertel et al., 2000; Bal and Oertel, 2000; Soares et al., 2002; Koch and Grothe, 2003; MacLeod et al., 2006; Nogueira et al., 2006; Nogueira and Caputi, 2011).

The first consequence of the combination of K$^+_{LT}$ with I_h is the emergence of a stable and low noise sensory device (Trussell, 1999; Carr et al., 2005). It is important to note that the presence of a K$^+_{LT}$ does not imply a unique molecular substrate; rather, different arrangements of molecular subunits may serve the same phenotype. In fact, while in auditory neurons dendrotoxin blocks low-threshold outward rectification (Bal and Oertel, 2001), our own research in the electrosensory system of *G. omarorum* shows that outward rectification is not affected by dendrotoxin (J.N. and A.A.C., unpublished).

Second, the combination of K$^+_{LT}$ and I_h increases the sensitivity to fast transients, supporting precise timing of the spikes and reducing temporal summation in the auditory system (Trussell, 1999; Koch and Grothe, 2003). This also shapes the frequency response of the onset neurons in *G. omarorum*. Best responsiveness is between 25 and 120 Hz. In *G. omarorum*, blocking the K$^+_{LT}$ current with 4-aminopyridine (4AP) dramatically reduces the cutting frequency of the high-pass arm of the filter (Fig. 2).

Third, in some systems, for example the fast electrosensory pathway of *G. omarorum*, the presence of the K$^+_{LT}$ conductance causes a reduction in cell excitability after subthreshold and suprathreshold depolarizations. Four lines of argument support this affirmation (Nogueira et al., 2006; Nogueira and Caputi, 2011): (1) subthreshold pulses of increasing intensities are followed by a reduction of the depolarization caused by a second pulse (Fig. 3A); (2) action potentials are followed by an increase in cell membrane conductance (Fig. 3B) and an increase of spike threshold (Fig. 3C) and (3) a long refractory period of similar time course (Fig. 3D); and (4) this long refractory period is reduced under the treatment with low doses of the K$^+$ channel blocker 4AP (compare Fig. 3D and 3E).

Similar to fish, the K$^+_{LT}$ channel observed in auditory cells of guinea pig (Manis and Marx, 1991) deactivates slowly, although to
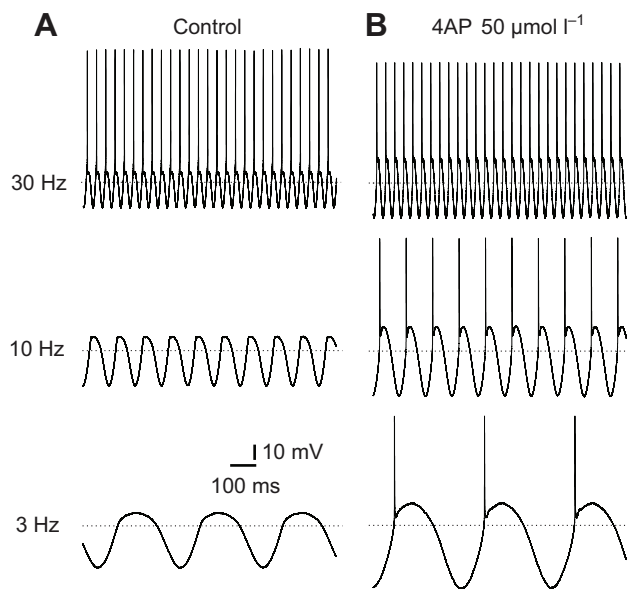
Fig. 2. Spherical neuron phenotype. Responses to sine waves of different frequency. (A) Considering spiking behavior only, the neuron responds as a band-pass filter, firing a single spike per cycle between 20 and 120 Hz. Only the low-frequency component of the band-pass filter is shown here. (B). The high-pass component was eliminated when potassium conductance was blocked with 50 µmol l⁻¹ 4AP. Dotted lines represent the resting membrane potential at −66 mV (stimulus: 0.9 nA peak to peak).

facilitates spike repolarization and accelerates deactivation of the low-threshold current, allowing the auditory onset cells to follow high-frequency stimuli (Bal and Oertel, 2001; Manis and Marx, 1991; Carr et al., 2001). Moreover, the relative weight of low- and high-threshold K⁺ currents has been found to be adapted to the role of the neuron; for example, the larger weight of high threshold conductance in the high-frequency region of the laminaris nucleus in the barn owl (Parameshwaran et al., 2001). Accordingly, there is also some evidence suggesting this variable association of low- and high-threshold K⁺ currents in spherical neurons of wave-type electric fish (Mehaffey et al., 2006). Interestingly, a recent article showed that spherical neurons of *Brachyhypopomus gauderio*, a slow electric organ discharge (EOD) rate pulse gymnotiform that shows large differences in sociality with *G. omarorum* (Silva et al., 2007), do not exhibit the low responsiveness window and the long refractory period observed in *G. omarorum* (Matsushita et al., 2012). In addition, it is likely that the expression of high threshold conductance in spherical neurons of the wave-type fish *Apteronotus* and *Eigenmannia* allows them to follow the relatively high frequencies of their EODs.

Fourth, one-spike-onset neurons show different degrees of synaptic convergence of afferent fibers depending on the system (Golding et al., 1995; Castelló et al., 1998). Differences in the innervation pattern and cell morphology are the basis of another computational mechanism that may decrease the responsiveness of the cell for asynchronous inputs. Bitufted coincidence detector neurons sharing low input impedance and K⁺$_{LT}$ channels occur in the auditory system of mammals, birds and reptiles (Carr et al., 2005). Depolarization generated by a given synaptic subthreshold current can only be effective for neuron firing when another synaptic current is added. In one-spike neurons this summation can only occur when the presynaptic afferent spikes fire within a short time window of each other (2 ms). Beyond this period a preceding

our knowledge the computational role of the refractory period in the one-spike-onset neurons of the auditory system is not yet well characterized. In other auditory cells there is a characteristic association of the K⁺$_{LT}$ with a high-threshold K⁺ conductance that
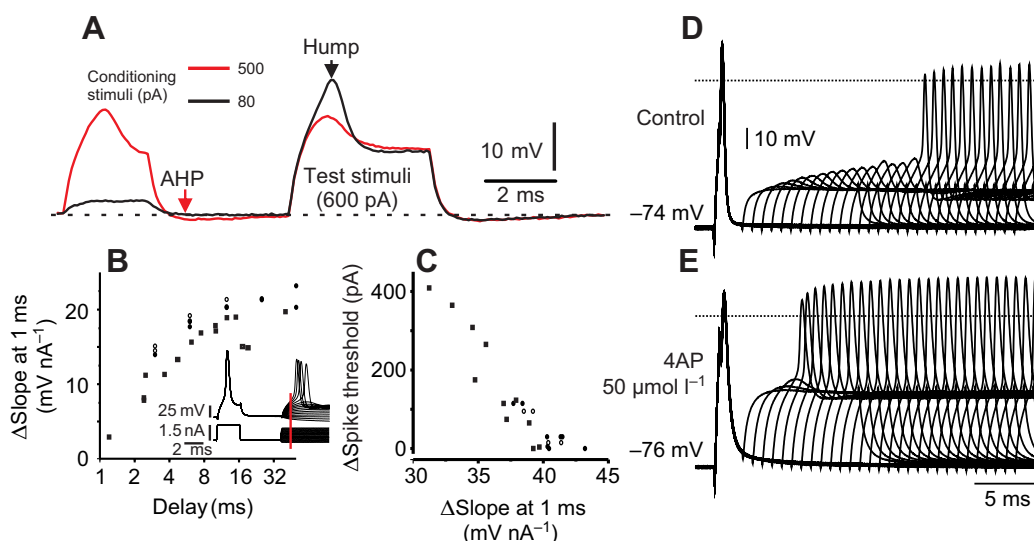

Fig. 3. Spherical neuron phenotype. A long refractory period is generated by a low-threshold K⁺ current. (A) K⁺ current is activated at subthreshold depolarizations. Subthreshold stimulation leads to an after-hyperpolarization (AHP; red arrow). Paired pulses cause a decrease in excitability evidenced by the reduction in the depolarization peak evoked by a constant amplitude test pulse (black arrow) following a conditioning pulse. (B,C) The long refractory period was evaluated by applying a series of current steps of different intensity at different delays, after a conditioning pulse evoking a spike (inset). The change in membrane conductance (B), evaluated as a change in the slope of the voltage–current plot obtained from values 1 ms after the onset (inset red line) and the excitability (C), evaluated as the change in spike threshold, are plotted as a function of the delay. (D,E) Long refractory period is substantially reduced by 4AP. (D). Superimposed traces obtained from paired pulse stimulation at different delays show the long-lasting refractory period. (E) This is substantially reduced by blocking the K⁺$_{LT}$ channel with 50 µmol l⁻¹ 4AP. Dotted lines indicate zero potential. A, D and E were modified from Nogueira and Caputi (Nogueira and Caputi, 2011); B and C were modified from Nogueira et al. (Nogueira et al., 2006).

depolarization causes a reduction of excitability (Fig. 3). Thus, multi-innervated one-spike-onset neurons may only respond to relatively synchronous afferent activities and their responsiveness could be strongly affected by a preceding spike. Although in the spherical neurons of *G. omarorum* the synaptic inputs are not anatomically segregated as in bitufted auditory neurons and these coincidence detection mechanisms are not yet demonstrated, these mechanisms may very well be present. In fact, one of the differences between the three somatotopic maps to which primary electrosensory afferents project is the number of synaptic contacts that each spherical neuron receives. This number increases from a single calyx in the centro-medial map to multiple club endings at the lateral map (Castelló et al., 1998). Analogously to the auditory neurons, intrinsic properties may endow multi-innervated spherical neurons of the lateral map of *G. omarorum*'s electrosensory lobe with the ability to perform precise coincidence detection.

Finally, one must note another potential common function of one-spike-onset neurons of auditory and electric senses. In pulse fish and also in the auditory system the signals are modulations of a non-continuous carrier. Encoding of words (Jusczyk, 1999) and pulse fish EODs (A. Rodríguez-Cattáneo, A. C. Pereira and A.A.C., unpublished data) (Bell et al., 1997a) is organized in discrete packages. Detecting the onset of each of these packages may be useful for central decoding of sensory messages, and syllable onset could be critical information for syllable decoding. This may be related to the role of the spherical neuron in the electrosensory lobe of *G. omarorum* as we describe next.

A one-spike-onset neuron in a specific circuit: the electrosensory lobe of electric fish

Electroreception is the ability to sense and communicate using electricity as a sensory carrier (Lissmann, 1958; Bullock et al., 1961; Scheich and Bullock, 1974; Kalmijn, 1974). Electroreception has two modes: passive (when the signals come from external sources) and active (in which signals are the modulations of a self-generated electric field). In passive electroreception, electric fields stimulating a cutaneous electrosensory mosaic may arise from real electric sources, for example, cutaneous, muscular or cardiac activities, or (in the case of electric fish) specialized electrogenic organs (EOs). In active electroreception, if the impedance of objects is different from that of the water, objects are polarized by the fish's self-generated electric field. Thus, objects behave as virtual electric sources in the same way that a planet or its satellites behave as virtual sources of light, when reflecting the sunlight (Lissmann, 1958; Lissmann and Machin, 1958). Nonetheless, instead of a DC source, the EOs of electric fish discharge repeatedly with a species-specific stereotyped waveform to which the electroreceptors of the species are tuned (Bastian, 1976; Watson and Bastian, 1979; Hopkins, 1976). This system organization in species-specific channels serves to optimize the signal to noise ratio while incurring the risk of potential jamming by the EOD of a conspecific neighbor (Caputi and Nogueira, 2012) (see below).

In electric fish, active and passive electric senses may share the same channel because EOD-generated fields have a dual function (Aguilera et al., 2001): (1) to carry self-generated electric images of the environment (so-called active electroreception) (Bennett, 1970; Bennett, 1971) and (2) to send communication signals to conspecifics (one form of passive electroreception) (Hopkins, 1974a; Hopkins, 1974b; Hopkins, 1999).

The ways in which self- and allo-generated images may interfere depend on the electric carrier type used by the fish. Evolution has converged on three main types of active electric carriers in the two main known groups of weakly electric fish, African mormyriforms and American gymnotiforms (reviewed in Moller, 1995): (1) brief electric pulses, irregularly emitted by a localized source (pulse mormyriforms); (2) a continuous sine-wave-like discharge generated by multiple sources having the same principal frequency component (wave mormyriforms and wave gymnotiforms); and (3) brief electric pulses resulting from the weighted sum of multiple sources generating specific time waveforms along the EO (pulse gymnotiforms).

These three strategies of active electric sensing are not only different on the motor side but are also different, in a corresponding manner, on the sensory side. Nonetheless, similarities, important for the understanding of this article, arise through convergent evolution in mormyriforms and gymnotiforms.

On the motor side, the most conspicuous common finding is that the EOD waveform is species-specific (Coates et al., 1954). The EOD has been likened to a fixed motor pattern that is driven one-to-one by the action of a command nucleus (Rodríguez-Cattáneo et al., 2008). In all species a command structure (so-called relay nucleus) projects and controls the recruitment of the electro-motor-neuron pools that drive the EO (Bennett, 1971; Dye and Meyer, 1986).

The repetition rate of the discharge of the EO is determined in a different way depending on the fish taxon. In pulse mormyriforms, the integration of the descending projections on a command and precommand nucleus causes an irregular discharge of the EO (Grant et al., 1986; Grant et al., 1999). This allows the fish to use an inter-EOD-interval sequence code to communicate (Carlson and Hopkins, 2004; Carlson, 2009).

In pulse gymnotiforms and all wave fish, descending neurons are driven regularly by the activity of an electrotonically coupled pacemaker nucleus (Dye and Meyer, 1986; Dye, 1987; Spiro, 1997; Moortgat et al., 1998; Moortgat et al., 2000). Prepacemaker neurons projecting on this nucleus determine either tonic or phasic modulation of the EOD rate (Watanabe and Takeda, 1963; Westby, 1974; Hopkins, 1974b; Dye and Heiligenberg, 1987; Kawasaki and Heiligenberg, 1988; Kawasaki et al., 1988; Curti et al., 1999; Curti et al., 2006; Post and von der Emde, 1999; Caputi et al., 2003; Comas and Borde, 2010) and changes in EOD waveform [sometimes acting on both pacemaker and relay neurons (Kawasaki and Heiligenberg, 1988; Engler and Zupanc, 2001; Perrone et al., 2009; Quintana et al., 2011)].

On the sensory side, at the first central sensory relay, the electrosensory lobe (ELL) located in the rhombencephalon of both African and American taxa, signals are split in two pathways that converge on mesencephalic structures (Szabo et al., 1975). There is a 'fast path' characterized by pauci-dendritic neurons interconnected by gap junctions and responding precisely phase-locked to every pulse or cycle of the EOD, and a more complex 'slow path' organized as a cerebellum-like circuit in which the number and/or probability of spikes of each cell type depends on the location of the cell in the circuit and the recent history of the signal flow (reviewed by Bell and Maler, 2005; Kawasaki, 2005).

While the fast electrosensory pathway follows the EOD reafferent signals without adaptation (Baker, 1980; Pereira et al., 2005), the slow pathway shows clear adaptive responses possibly serving novelty detection, among other functions (Bell, 1981; Bell et al., 1993; Bastian, 1986a; Bastian, 1986b; Bastian, 1995; Bastian, 1999; Bell et al., 1993; Bell et al., 1997a; Bell et al., 1997b; Lewis and Maler, 2002; Grau and Bastian, 1986; Pereira et al., 2005; Caputi et al., 2008). Here we focus on the one-spike-onset neurons representing the fast pathway in the electrosensory lobe.

In pulse gymnotiforms the neurons of the ELL respond to the self-generated electric field with a well-defined pattern of discharge. While the fast electrosensory pathway carries a latency encoded image of the head region (Castelló et al., 1998), the slow pathway shows different neuron types characterized by a post-EOD probability pattern of discharge (A.A.C., unpublished).

The fast electrosensory pathway was described by Thomas Szabo in gymnotid and mormyrid fish (Szabo, 1967; Szabo et al., 1975). In *Gymnotus* it originates in tuberous electroreceptors located predominantly in the head region (so-called pulse marker afferents) (Bennett, 1967; Bastian, 1976; Watson and Bastian, 1979). The transcutaneous field evoked by the EOD at the receptor pore triggers a spike at its single arising afferent neural fiber (Bennett, 1967; Watson and Bastian, 1979; Yager and Hopkins, 1993). This spike follows the EOD with an amplitude dependent latency (Szabo et al., 1975; Watson and Bastian, 1979). In consequence, the afferent population encodes the image of nearby objects as a pattern of relative latencies.

Pulse marker receptor organs are distributed over the head increasing in density at the center of the jaw, where electroreceptor density and variety are maximal (Castelló et al., 2000). This zone also has the relatively largest representation in the electrosensory lobe (Castelló et al., 1998) and receives electrosensory images with the highest contrast (Caputi and Budelli, 1995; Castelló et al., 2000; Caputi et al., 2011). Taking into account the anatomical and functional similarities with the foveal region of the vertebrate eye (Ramón y Cajal, 1899), the lips and fingertips of primates (Penfield and Boldrey, 1937; Jain et al., 1998), the vibrissae pad in rodents (Lorente de Nó, 1922) and other specialized regions of sensory systems (Catania and Kaas, 1997; Catania et al., 2000), this region has been likened to an electrosensory fovea (Castelló et al., 2000; Bacelo et al., 2008).

Pulse markers project on pear-shaped or spherical somata typical of the three tuberous maps of the ELL. Spherical neurons are scattered along the border between the neuropil and the ganglion cell layers in the lateral, centro-lateral and centro-medial maps, but are absent in the medial map receiving the ampullary receptors (Réthelyi and Szabo, 1973; Castelló et al., 1998). Synaptic contacts between pulse markers and spherical neurons are different depending on the electrosensory map, implying different degrees of convergence (Castelló et al., 1998). Electron microscopy revealed mixed synapses in all cases (Castelló et al., 1998).

In most pulse gymnotids, spherical neurons project onto a medial mesencephalic nucleus magnocellularis in which two types of cells have been described according to their size and synaptic contacts. The large neurons (from which this nucleus takes its name) show multiple processes contacting the small cells, which, in turn, project onto the torus semicircularis (Sotelo et al., 1975; Matsushita et al., 2012). The magnocellular mesencephalic nucleus was postulated to be a coincident detection circuit (Szabo, 1967; Schlegel, 1973; Matsushita et al., 2012).

Due to the one-spike onset response characteristic of the pulse markers and spherical neurons, the population activity evoked by the self- and allo-generated EODs can be recorded as a compound action potential at the nerve, ELL, lateral lemniscus and mesencephalic magnocellular nucleus (Castelló et al., 1998; Nogueira et al., 2006; Nogueira and Caputi, 2011) either in acute experiments or in chronically implanted freely moving fish. The changes in the self-generated local EOD introduced by the presence of objects modulate the firing latency of the pulse marker and spherical neuron axons. This results in changes in amplitude and width of the field potential measured in the lateral lemniscus and

in the nucleus magnocellularis. Global increases of the electric field as observed when the fish is inside a plastic tube are pulse to pulse, linearly related to the increment in amplitude of the local EOD. This indicates that there is no adaptation in afferent or second-order neurons (Pereira et al., 2005).

The EOD of a second fish is also able to recruit the fast electrosensory pathway. The amplitude of the compound potential measured in the lateral lemniscus and in the nucleus magnocellularis is dependent on distance and position between fish (as it is expected by the change in the amplitude of the allo-generated electric image). Interestingly, even when both fish remain in a steady relative position, the stimulus–response relationship depends on the interval between the self- and allo-generated EODs (Fig. 4) (Castelló et al., 1998; Nogueira et al., 2006; Nogueira and Caputi, 2011). Within a time window lasting approximately 5–10 ms after the self-generated EOD, the axons of spherical neurons recorded in the lateral lemniscus and the neurons of the nucleus magnocellularis do not respond to further peripheral stimuli (Fig. 4, frame 1, the artifact of the allo-generated EOD is marked as 'a'). Beyond this absolute window, responsiveness gradually increases with the delay between stimuli (Fig. 4, frames 2 to 5). This was called the low responsiveness window of the fast electrosensory pathway (Castelló et al., 1998).

When the compound action potential was recorded simultaneously at the mandibular nerve and the lateral lemniscus, the interval dependence was only observed in the latter, indicating the presence of a sensory filter in the electrosensory lobe (Castelló et al., 1998). This filter is not implemented by an inhibitory, internally generated, expectation signal coming from the motor commands (i.e. a corollary discharge), as was shown by the constancy in amplitude of the response to an electric stimulus applied without temporal relationship in curarized fish (Castelló et al., 1998). A paired-pulse study in curarized fish showed that the
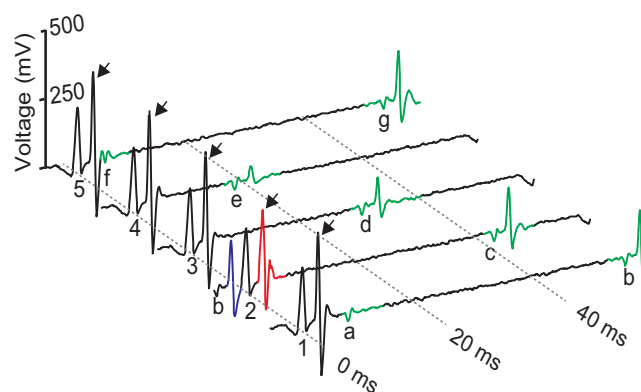

Fig. 4. The low responsiveness window of the fast electrosensory pathway. Field potentials evoked by the self-generated and conspecific-generated electric organ discharges (EODs) recorded in the magnocellularis nucleus in a freely moving fish. The self-generated EOD triphasic artifact (labeled 1–5 around time zero in each trace) is followed by a spike (arrows) corresponding to the evoked response. The conspecific-generated EOD artifact is the small triphasic waveform highlighted in green (labeled a–g). The response evoked by the conspecific-generated EOD (green spikes following the artifact) is absent at short delays (a and f) and increases in amplitude with the interval between the self-generated EOD and the conspecific-generated EOD (green evoked spikes labeled e, d, c and b). Note that a similar, but smaller, decrease in the response to the self-generated EOD is provoked by the activation of the fast electrosensory pathway when the conspecific-generated response (second trace, blue spike) occurs just before the self-generated EOD (red spike). Modified from Nogueira et al. (Nogueira et al., 2006).

larger the conditioning stimuli, the larger the reduction of the response to a constant test stimulus (Castelló et al., 1998). These characteristics of the response and the presence of *en passant* boutons showing oval vesicles characteristic of inhibitory chemical synapses suggested the possibility of a feed-forward inhibition as the mechanism of this signal filtering in the ELL (Castelló et al., 1998). Although one cannot rule out this complementary hypothesis at this time, more recent research indicates that the main factor underlying the low responsiveness window is the response function of the spherical neurons, described next.

Spherical neurons show a one-spike phenotype (Soares et al., 2002), as shown by whole-cell patch recordings in brain slices of the electrosensory lobe (Nogueria et al., 2006; Nogueira and Caputi, 2011) (Fig. 1). This suggests the presence of a low-threshold, non-inactivating K^+ conductance and a hyperpolarization-activated I_h. Confirming this view, pharmacological studies show that very low doses of 4AP turn the typical one-spike response into a repetitive firing profile and the depolarization sag characteristic of I_h during hyperpolarizing stimuli is blocked by CsCl (J.N. and A.A.C., unpublished). Furthermore, there is a marked increase of action potential duration under low doses of 4AP that contrasts with a minimal increase in action potential duration caused by tetraethylammonium, indicating that subthreshold activity, as well as action potential repolarization, depends on the presence of the K^+_{LT} channel (J.N. and A.A.C., unpublished). Last, but not least important, K^+_{LT} expressed by spherical neurons is insensitive to a broad range of dendrotoxin doses, suggesting that another conductance insensitive to these drugs may be also important for the outward rectification and/or that the K^+_{LT} channel might belong to an as-yet-undescribed type (J.N. and A.A.C., unpublished).

The K^+_{LT} conductance appears to be the main cause of the low responsiveness window observed in the field potentials recorded *in vivo*. In fact, the amplitude of the compound action potential response depends on the number of spikes provoked by the stimulus and the degree of synchrony between them. In the case of two successive stimuli, the amplitude of the second compound action potential is reduced for three reasons: (1) when the interference occurs at short delay after the EOD, it causes a lack of cell response (Fig. 5A); (2) between the fully non-responsive period and the fully responsive state there is an interval where the response has different degrees of probability (Fig. 5A,C, top); and (3) the spike latency and latency variability show a clear reduction as this interval is increased (Fig. 5B,C, middle and bottom).

Finally, it must be taken into account that the self-generated EOD is much stronger and spatially more evenly distributed than a conspecific EOD. The electric image of a conspecific is lateralized on one side of the fish's body (A. Rodríguez-Cattáneo and A.A.C., unpublished). The partial activation of the population of receptors of the fast electrosensory pathway further contributes to the global reduction of the amplitude of the field potential caused by a conspecific EOD, occurring after the self-generated EOD.

Summing up, the last three arguments explain that the average responses of a neuron to test stimuli applied intracellularly *in vitro* at different delays after a conditioning one would reproduce the response of the cell population obtained *in vivo* (Fig. 5D,E). In both cases, *in vivo* and *in vitro*, the refractoriness was blocked by 4AP (Fig. 5F,G). The crucial role of this long refractory period for favoring self- over allo-generated signals results from the analysis of the neuron responsiveness under a particular functional context.
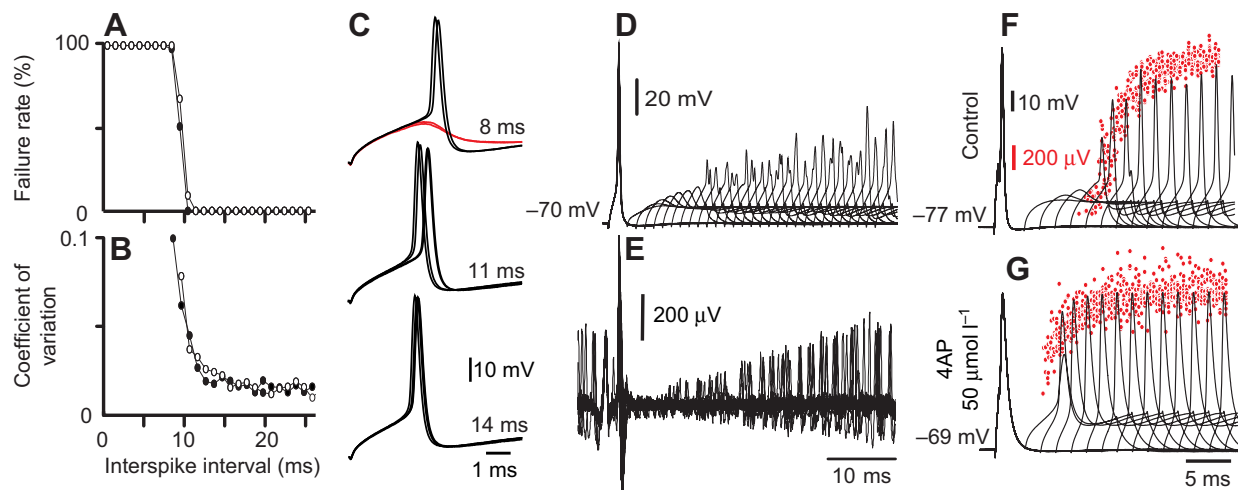

Fig. 5. Cellular basis of the low responsiveness window. (A) Spike failure rate and (B) spike latency variability are plotted as a function of the interval between pulses following a natural sequence of intervals (open and filled circles were obtained from the same neuron using two sets of intervals) (for details, see Nogueira and Caputi, 2011) (C) Raw traces from another neuron illustrate spike latency variability at 8 (top, note the failures in red), 11 (middle) and 14 ms (bottom). (D) Failure rate and latency variability determine that the averaged responses increase with the interstimulus interval (each overlapped trace corresponds to the average of 10 runs of paired pulse stimulation experiments in the same cell). (E) Field potential traces obtained in the nucleus magnocellularis of a chronically implanted fish are shown overlapped. The large spikes at the beginning are the responses to the fish's own EOD. Responses to a conspecific EOD increase in amplitude as the interval between the self- and the allo-generated EOD is increased. Thus averaged responses of a single cell resemble the averaged responses of the cell population. (F,G) *In vivo* and *in vitro* phenomena are equally affected by the K^+ channel blocker 4AP. (F) Averages of whole cell patch recordings from spherical neurons stimulated with paired pulses applied at increasing intervals (each superimposed black trace corresponds to the average of five runs of paired pulse stimulation experiments in the same cell) are superimposed with red dots representing the peak-to-peak amplitude of the field potentials evoked by a conspecific EOD. (G) 50 µmol l^{-1} 4-AP treatment (each overlapped black trace correspond to the average of five runs of paired pulse stimulation experiments in the same cell) causes a similar effect as the injection of 4AP in the cisterna magna (red dots). A and B were modified from Nogueira and Caputi (Nogueira and Caputi, 2011); D and E were modified from Nogueira et al. (Nogueira et al., 2006).

The computational task: the tradeoff between self- and allo-generated signals

As in all active senses, electroreceptors of a given species are tuned to the dynamic range of the species-specific signal carrier. Because such a dynamic range may be shared by externally generated events (in particular by the electric field generated by conspecifics), fish have developed different mechanisms to separate self- from allo-generated signals flowing through the same sensory channel. Before focusing on the role of the one-spike spherical neurons of the fast electrosensory path, during active electric sensing in the presence of the interference signals, we will first briefly describe the main strategies shown by electric fish for dealing with self-generated signals in the presence of allo-generated signals.

The simplest and most effective way of separating self- and allo-generated signals is to create a self-generated expectation signal in one's own sensory system (Sperry, 1950; von Holst and Mittlestead, 1950). This is called in general corollary discharge (Sperry, 1950). It is a motor-driven signal that is integrated with sensory input. According to the different levels of integration along the sensory–cognitive path, corollary discharges have been subclassified into different subtypes (Crapse and Sommer, 2008).

In pulse mormyrids, self- and allo-generated signals are clearly separated by corollary discharges. In these fish the fast electrosensory pathway arises from a single type of very sensitive electroreceptors (knollenorgans), innervated by thick myelinated fibers discharging a single spike per EOD. These fibers make electric synaptic contacts with the cells of a compact cell group in the rhombencephalon, the nucleus of the electrosensory lobe. In addition to these synaptic contacts, the cells of this nucleus also receive multiple GABAergic contacts from a mesencephalic relay of the corollary discharge. These contacts provoke a strong inhibition, completely blocking self-generated signals but allowing the arrival of signals evoked by the EOD of a conspecific, seldom falling within the inhibitory window (Bell and Grant, 1989; Bell et al., 1995). Thus the fast pathway of pulse mormyryforms is a private channel only responding to allo-generated signals. There is no evidence of a corollary discharge in gymnotiforms and wave mormyriforms; thus, nature evolved more complex mechanisms for avoiding the interference (Kawasaki, 2005).

In wave fish, the interference from another wave fish discharging at a similar frequency is potentially disadvantageous for active electrosensing, because a small frequency difference causes a frequency beat or 'terzo suono' (Tartini, 1754; Chialvo, 2003) that would appear as a relatively slow change in the amplitude of the signal (Watanabe and Takeda, 1963; Bullock et al., 1972; Bullock et al., 1975) (reviewed by Heiligenberg, 1991). This generates a 'phantom' image comparable to the image of a moving object. The magnitude of the disadvantage increases as the frequency decreases, and more importantly, depending on the fish's relative position, may not be the same at all places of the sensory mosaic. To solve this ambiguity, wave fish evolved a complex circuitry involving several structures of the mesencephalon and diencephalon (Carr et al., 1986a; Carr et al., 1986b; Carr and Maler, 1986). The output of the last stage of this circuitry, the nucleus electrosensorius, projects onto prepacemaker structures controlling the discharge frequency of the pacemaker nucleus driving the EOD cycle (Heiligenberg and Rose, 1985; Heiligenberg and Rose, 1986; Rose and Heiligenberg, 1986; Keller and Heiligenberg, 1989; Keller et al., 1990; Kawasaki, 1996). By shifting the frequency of their own EODs in opposite directions, a pair of fish is able to increase the frequency difference and to reduce the ambiguity. This response was called the jamming avoidance response of wave fish (Watanabe and Takeda, 1963; Bullock et al., 1972; Bullock et al., 1975; Heiligenberg, 1991; Kawasaki, 1996) and it is one of the best-known neuroethological examples in which a complex behavior is explained on the basis of the precise knowledge of the subservient neural network.

Instead of the tonic shift in pacemaker activity frequency characteristic of the jamming avoidance of wave fish, pulse gymnotiforms, apparently lacking corollary discharges, respond to the interference with two main behaviors characterized by transient accelerations of the pacemaker activity (Bullock, 1969; Westby, 1974; Westby, 1979; Westby, 1981; Capurro et al., 1998; Capurro et al., 1999) (Fig. 6A). These transient shortenings of approximately 2–10% of the inter-EOD interval occur during active exploration (Jun et al., 2012), immediately after detecting a novel stimulus (Caputi et al., 2003), in the presence of other fish (Bullock, 1969; Westby, 1974; Westby, 1979; Westby, 1981; Capurro et al., 1998; Capurro et al., 1999) and during escape responses (Curti et al., 1999; Curti et al., 2006).

In the presence of interference, two patterns of discharge can be identified in the inter-EOD interval. These patterns are better understood when the phase of the interference signal and the inter-EOD interval are plotted together as a function of time. One pattern is the jamming avoidance response (Fig. 6A, left side of the plot) and is characterized by repetition of transient reductions of the inter-EOD interval followed by a smooth relaxation course. During jamming avoidance periods the phase continuously increases. In contrast, there are 'synchronization bouts' in which the rate of the self-generated EOD and the allo-generated events have the same mean rate, and the phase oscillates in the first half of the inter-EOD interval (Fig. 6A, right side of the plot) (Westby, 1974; Westby, 1979). During synchronization bouts the phase is reduced up to the point that a collision occurs, and then the transient acceleration of the pacemaker activity causes an increase in the phase. When the inter-EOD interval overcomes the interval between interference pulses, the phase is again reduced, starting a new cycle.

To explain this process, we define one dynamic cycle for each behavior. In each cycle, five stages can be recognized (Fig. 7A).

Stage 1: When the allo-generated events occur with a short phase delay, the receptors of the slow electrosensory pathway are still in their refractory period.

Stage 2: Adaptation of peripheral receptors in the slow pathway reduces the interference acceleration effect on the pacemaker activity and the inter-EOD interval increases (Baker, 1980; Baker, 1981). At the same time, the long-lasting refractory period of the spherical neurons blocks the interference signals in this pathway (green zone).

Stage 3: There is a bifurcation point depending on the difference between the rates of the EOD and the interference. If the phase is still within the adaptation period of the receptors originating the slow pathway when the inter-EOD interval becomes larger than the interval between interfering events, the phase is reduced, leading to synchronization bouts (blue trace in Fig. 7B). In contrast, if the phase of the interference is long enough to cause accelerations of the pacemaker activity when the inter-EOD interval is smaller than the interval between interfering events, the interval is reduced as the phase increases. This leads to jamming avoidance responses.

Stages 4 and 5: These are different in each behavior. While during Stage 4 in synchronization bouts the phase continues to decrease due to the lack of effect of the interference on self-generated signals, during Stage 4 of jamming avoidance responses (red trace in Fig. 7B) the effect of the interference on self-generated signals causes an increase in the rate of pacemaker activity. At
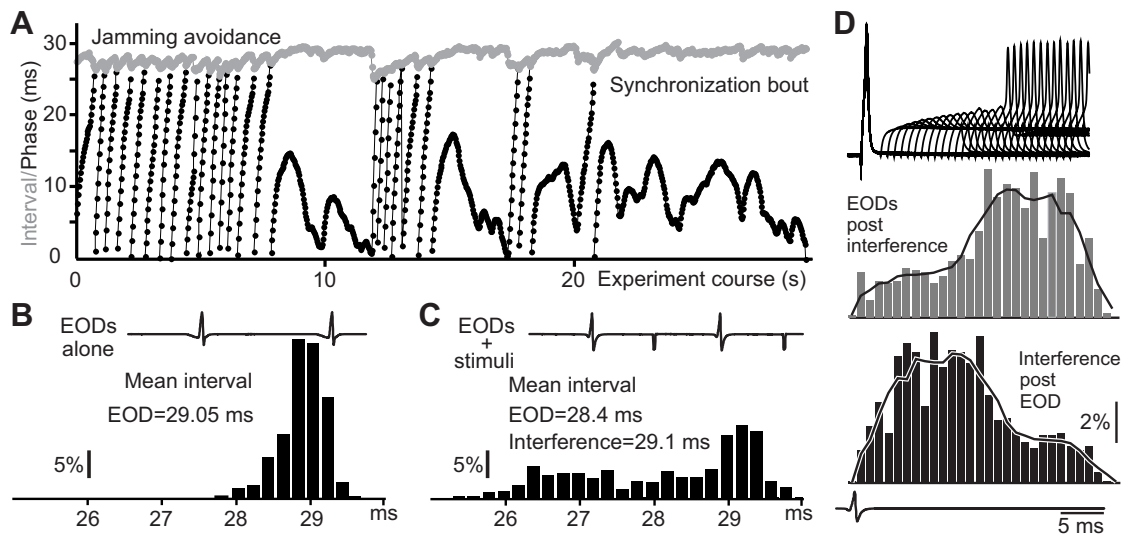
Fig. 6. The active electrosensory task. Hypothetic sensory role of the spherical neurons during electrical interactions of two fish. (A) Pacemaker behaviors in the presence of a regular train of interfering electrosensory events. Gray dots represent the series of inter-EOD intervals and black dots represent the phase of the interfering stimuli. Two different behaviors are shown: (1) jamming avoidance responses are characterized by a sweep of the interval due to an interfering stimulus progressively increasing in phase and a series of transient accelerations of the EOD rate; (2) synchronization bouts occur when the rate of the EOD is lower than the rate of the interference. (B) First-order inter-EOD intervals at rest. (C) First-order inter-EOD intervals under interference showing an increase in skewness. (D) Hypothesized computational role of spherical cells during fish interaction with allo-generated electrosensory events. The panel compares the refractory period of an intracellularly recorded single neuron (as shown by paired pulse stimulation, see Figs 4, 5) with the probability of interference after the EOD (gray bars; the zero interval is defined as the moment of fish's EOD) and the probability of the EOD after the interference (black bars; the zero interval is defined as the moment of the interference pulse). Overlapped lines show the smoothed version of the histograms. These distributions suggest that the refractory period blocks the allo-generated stimuli more strongly than the self-generated ones. Modified from Caputi and Nogueira (Caputi and Nogueira, 2012).

Stage 5 of synchronization bouts there is a collision between the self-generated EOD and the interference, causing a novelty-like stimulus with the consequent pacemaker activity acceleration (Westby, 1974). During most of the synchronization bout cycle the fast electrosensory pathway barely detects a conspecific as a consequence of the long refractory period (green zone). At Stage 5 of jamming avoidance responses the pacemaker activity accelerates progressively as the interval between the interference and the EOD is reduced. Only within Stages 4 and 5 of the jamming avoidance responses may the fast electrosensory pathway be able to detect a conspecific (pink zone). When the phase reaches the next EOD, the cycle starts again (red dotted line).

The increase in the tendency to accelerate the pacemaker activity during these behaviors causes a skewing of the inter-EOD interval histogram to shorter intervals (Fig. 6B,C). The transient reduction in responsiveness of the slow pathway receptor subtypes causes neural signal reduction that, in turn, triggers the transient accelerations of pacemaker activity (Baker, 1980; Baker, 1981; Heiligenberg et al., 1978). This causes, in turn, a late electrosensitive phase in the inter-EOD interval in which repetitive stimulation may cause pacemaker activity accelerations (Bullock, 1969; Westby, 1974; Westby, 1979; Westby, 1981; Capurro et al., 1998; Capurro et al., 1999). As a consequence, coincidence over successive EODs is reduced (Heiligenberg et al., 1978; Capurro et al., 1999). It has been shown that the same dynamic process can explain both synchronization bouts as well as jamming avoidance responses (Fig. 7B) (Caputi, 2012). In fact, during jamming avoidance, accelerations (red line in Fig. 7B) occur when the allo-generated stimulus falls just before the EOD, causing a change in the response to the fish's own EOD of the receptors that originate the slow electrosensory pathway (Baker, 1980; Baker, 1981).

Synchronization bouts (blue line in Fig. 7B) occur when internal drives on the pacemaker nucleus diminish and the mean rate of the EOD becomes smaller than the rate of the external events. In this case the interference falls within a low responsiveness period of both pathways. Then the phase is progressively reduced up to the point that a coincidence evokes a novelty-like response.

This classic view of jamming avoidance focuses on prediction of imminent coincidences that would distort the reafferent signals (Heiligenberg et al., 1978). Notwithstanding, one should point out that even in the absence of coincidence, the intercalated self- and allo-generated spikes of the afferent population convey the simultaneous information from self-generated images and communication signals originated by conspecifics. Thus, only avoiding coincidences does not rule out major interference because the two images (self- and allo-generated) are simultaneously encoded by spikes of identical shape flowing intercalated through the same physical channel. Therefore, to understand the sensory consequences of this active control of the EOD, one has to explore the functional expression of neuron-intrinsic properties of the electrosensory pathways. Next, we focus on the spherical neurons of the fast electrosensory pathway.

The spherical neurons favor self-generated information
The pulse marker population encodes, as a relative latency map, the electric images projected on the fish's head. Self-generated images of the surroundings are intercalated with weaker conspecific-generated images. These two images are encoded as two respective latency patterns that reflect the intensity distribution of self- and allo-generated electric fields on the skin. Importantly, spikes corresponding to the two images are intercalated in time in the output firing of each individual primary afferent.
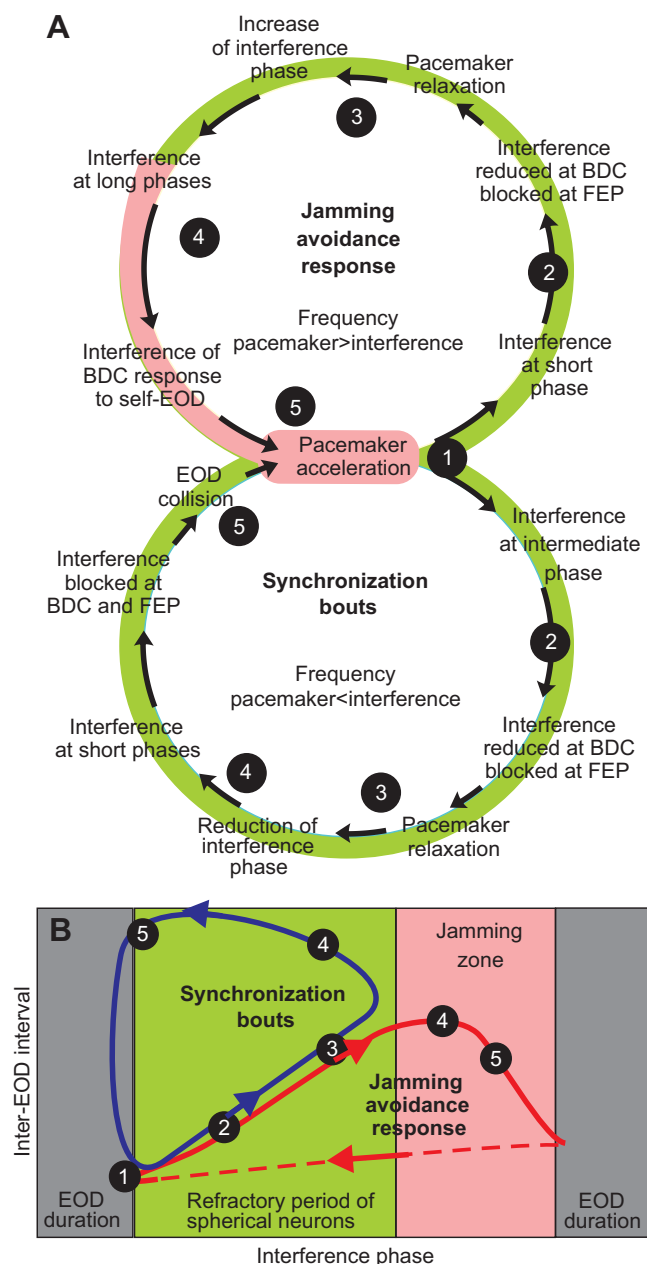
Fig. 7. Representation of the variations in the streaming of self-generated sensory signals. (A) The phase of the interference and the EOD interval are related by a double cycle. The uppermost cycle, occurring when the interference rate is smaller than the EOD rate, leads to jamming avoidance responses. The lower cycle, occurring when the EOD rate is smaller than the interference rate, leads to synchronization bouts. BDC, burst duration coder type of electroreceptors; FEP, fast electrosensory pathway. (B) Phase plot of the process representing the inter-EOD interval as a function of the interference phase. See the description of stages in 'The computational task: the tradeoff between self- and allo-generated signals'.

In order to understand how the spherical neurons favor self- over allo-generated signals, let us consider initially the neural image in the centro-medial map of the electrosensory lobe where afferent projection on the spherical neurons is nearly one to one. In this map, the spherical neuron refractory period blocks the response to an afferent spike at short latencies after the EOD. After this 'failure' period there is a second period (between 12 and 15 ms) in which spike latency would have important variations because the input is close to threshold. Finally, at longer delays the neuron responds with a single spike precisely timed to the sensory input (Fig. 6D, top).

In the case of multi-innervated cells, one must consider additionally that self-generated signals presumably almost always evoke a spike (Watson and Bastian, 1979). Thus, the effect of refractoriness on allo-generated responses will always be present, reducing the probability of spiking. Reduced probability of afferent spiking will lower the probability that spherical cells of the centro-lateral map will fire, because their higher convergence ratio implies a higher spike threshold. This effect will be even more pronounced in the lateral map that shows the highest convergence ratio of the three maps.

Considering that the amount of information preserved by the spherical neurons' response is dependent on the interval between signals of different origin (self- and allo-generated), one may hypothesize that the EOD rate accelerations adapt the intervals between different stimuli in order to make information transmission more efficient for self-generated electrosensory signals than for allo-generated signals. The phase (Fig. 6D, middle panel) and cophase (Fig. 6D, interval between allo- and self-generated stimuli, lower panel) histograms indicate that the probability of allo-generated events peaks just after the EOD and the probability of EOD peaks a few milliseconds before the next allo-generated event (Nogueira and Caputi, 2011). A key point of this hypothesis is that the modulation of the pacemaker intervals tends to avoid the refractory effects of allo-generated on self-generated signals and increase the refractory effects of self-generated on allo-generated signals. This is more marked for synchronization bouts than for jamming avoidance responses [see fig. 2 in Caputi and Nogueira (Caputi and Nogueira, 2012)].

We tested this hypothesis in two ways. First we asked whether an *in vitro* recorded spherical neuron stimulated with a natural pattern would respond more faithfully to the stimulus timed to the EOD than to the stimulus timed to the allo-generated event. Second we compared the amplitude variability of the field potentials evoked by the EODs and a series of allo-generated stimuli of constant amplitude during the jamming avoidance and synchronization bouts shown by chronically implanted fish.

In the *in vitro* experiments, we intracellularly played back stimulus patterns on spherical cells of the centro-medial and centro-lateral maps. Patterns of stimulation were obtained from behavioral experiments and consisted of time series of events in which each event corresponded either to a self-generated EOD (refered to as self-timed stimuli) or to the allo-generated interference pulse (referred to as allo-timed stimuli). Then, we analyzed separately the responsiveness of the spherical neurons to self-timed and allo-timed stimuli. To do this we separated the responses off-line according to their (self- or allo-) timed condition and dealt with each series of responses separately.

Intracellular stimuli were constant in amplitude and duration; therefore, in the absence of a timing effect the spike probability and spike latency histogram should be the same across phase delay. This was confirmed experimentally (Nogueira and Caputi, 2011). As described above, most allo-timed stimuli fall at short phases after the self-timed stimuli and most allo-timed stimuli fall at short co-phases before the self-timed stimuli. As a consequence, the spike latency dispersion and the spike failure rate to allo-timed stimuli are globally larger than those to self-timed stimuli (Fig. 8). In Fig. 8A,B, spike latency rasters are compared, showing that the response to self-timed stimuli is less variable that the response for allo-timed stimuli. The increase in dispersion of the resulting spike

latency histogram normalized by the number of stimuli quantifies the information lost at the level of spherical neurons for each stimulus series (Borst and Theunissen, 1999). Therefore, the degree of dispersion of the histogram of amplitudes is indicative of the loss of information. The spikes evoked by self-timed pulse show a sharper histogram (Fig. 8C) with larger area than the corresponding histogram for response to allo-timed stimuli (Fig. 8D). This is due to the differences in spike failure rate and latency variability.

In control experiments, a newly constructed stimulus train substituting self-timed stimuli by pseudo-self-timed stimuli with the same intervals as the self-timed stimuli, but shuffled in order, was applied to the same neuron. This maintains the same rate for the global stimulus train but disrupts the phase relationship between allo-timed and pseudo-self-timed stimuli. In these experiments, the increase in spike failure rate and the spike latency coefficient of variation showed no difference and their values were intermediate between those obtained for self- and allo-timed stimuli applied in a natural sequence. In Fig. 8E,F, spike latency histograms for pseudo-self-timed stimuli (filled bars) are compared with the histograms obtained using a stimulus train in which the same intervals were used but randomly altered in order (superimposed stairs). The smallest increase in histogram dispersion corresponds to self-timed stimuli and the largest increase corresponds to the allo-timed stimuli (Nogueira and Caputi, 2011). These results indicate that the amount of information loss at the spherical neuron level is larger for allo- than for self-generated signals. Because the neuron and the current pulses were identical for allo- and self-timed stimuli, the difference in information transfer is due to EOD timing.

In the *in vivo* experiments, we recorded the field potential evoked by the EOD and the allo-generated stimuli in chronically implanted, spatially restrained but freely discharging fish, at the nucleus magnocellularis. Chronically implanted fish perform the same behaviors described when an interference was presented though brief stimuli, regularly spaced at the same mean rate as the pacemaker (Fig. 9A). In these conditions, the amplitude of the field potential responses results from the summation of the individual action potentials, thus reduction of the amplitude would indicate an increase either in spike failure rate or in spike latency variability. As shown in Fig. 9B, the amplitude of the responses evoked by allo-generated stimuli is approximately 10 times more variable than the responses evoked by self-generated stimuli (Fig. 9C), confirming *in vivo* that the combination of the refractoriness of the spherical neurons and the EOD rate allows privileged information transmission for self-generated signals.

Conclusions

Comparative analysis indicates that the widespread type of vertebrate neurons referred to as the one-spike-onset phenotype is based on a similar, but not identical, repertoire of ionic conductances in which a low-threshold potassium current is crucial. Commonalities and differences between one-spike-onset neurons in the auditory system of birds and mammals and spherical neurons of electric fish indicate that, although belonging to the same general phenotype, one-spike-onset neurons show variation in their intrinsic properties adapted to the sensory task. This opens the question whether one-spike-onset neurons of auditory and electrosensory systems are homologous (and hence appeared very early during vertebrate evolution) or result from evolutionary convergence.

Commonalities between these neurons in different systems are their role for timing precision and coincidence detection. Differences are also observed in the tuning of each neuron type to
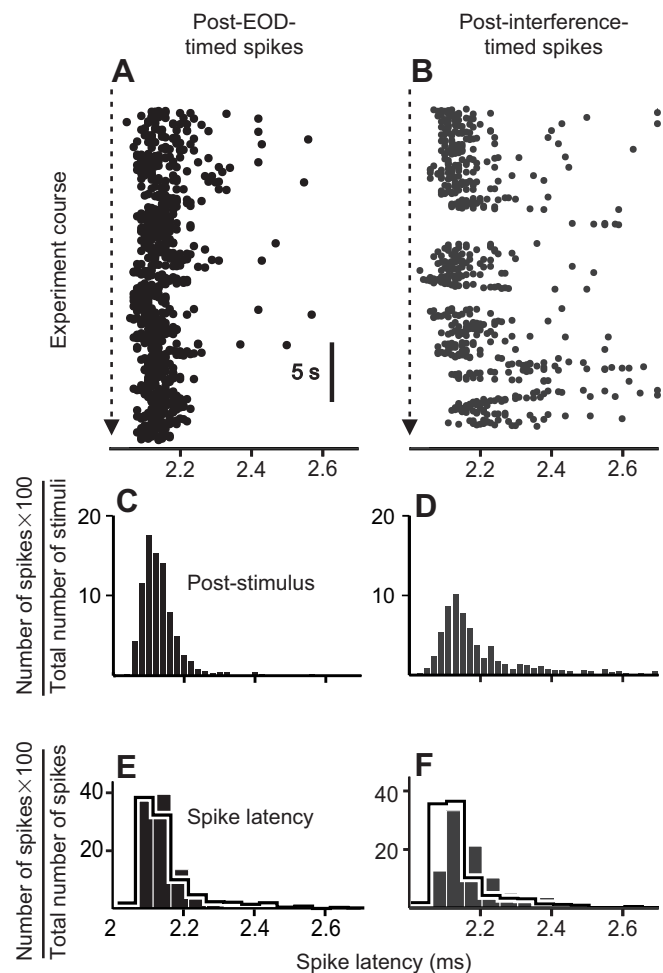

Fig. 8. Test of the hypothesis that the EOD rate accelerations adapt the intervals between different stimuli in order to make information transmission more efficient for self-generated electrosensory signals than for allo-generated signals. *In vitro* experiments. Results obtained from a single cell stimulated by a train of pulses timed as the self-generated EOD and an artifical pulse (allo-generated event) recorded during a behavioral experiment as in Fig. 6. (A) Post-stimulus raster plot of the spiking responses to self-timed pulses. (C) Corresponding post-stimulus histogram (ordinate: 100×EOD evoked spikes per bin divided by total number of EOD-timed stimuli). (E) The responsiveness to the natural pattern of stimuli (bars) is compared with the responsiveness to the same set of intervals applied in a shuffled sequence in a pairwise experiment (staircase histograms). For the sake of clarity, spike latency histograms, showing the relative frequency of latency values, were constructed with a different bin size (ordinate: 100×EOD evoked spikes per bin divided by total number of EOD evoked spikes). (B) Post-stimulus raster plot of the spiking responses to interfering pulses timed. (D) Corresponding post-stimulus histogram (ordinate: 100×interference evoked spikes per bin divided by total number of interference-timed stimuli, black bars). Note the larger dispersion of the histogram in A compared with the histogram in B. (F) The responsiveness to the natural pattern of interfering stimuli (bars) is compared with the responsiveness to a new train in which the self-generated intervals were substituted by a series of stimuli having the same interval probability but applied in a shuffled sequence (staircase histograms). For the sake of clarity, spike latency histograms, showing the relative frequency of latency values, were constructed with a bin size different from middle intervals (ordinate: 100×EOD evoked spikes per bin divided by total number of EOD evoked spikes). Reproduced from Nogueira and Caputi (Nogueira and Caputi, 2011).

its precise function. One of these differences expressed in *G. omarorum* is the use of the long-lasting refractory period to favor the information transmission of self-generated electrosensory
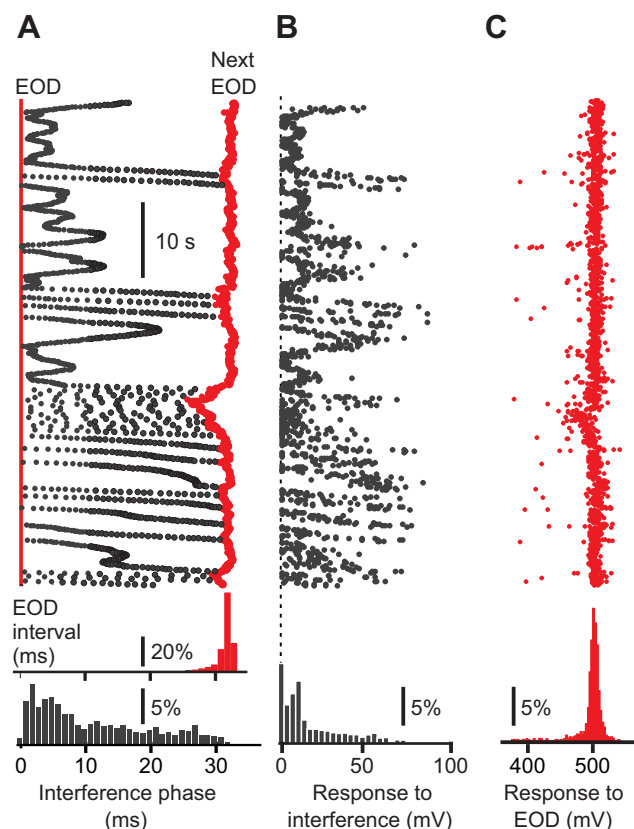
Fig. 9. Test of the hypothesis that the EOD rate accelerations adapt the intervals between different stimuli in order to make information transmission more efficient for self-generated electrosensory signals than for allo-generated signals. *In vivo* experiments. Field potentials evoked by self- and allo-generated events in the magnocellular nucleus of freely discharging fish dealing with interference. (A) The raster plots show the time course of the phase of interfering stimuli (black) and the successive intervals between EODs (red). Histograms at the bottom show the relative frequency of interference after the EOD (black bars, ordinate: 100×number of allo-generated stimuli per bin divided by the total number of EODs) and the first-order inter-EOD interval histogram (red). The zero interval is defined as the moment of the fish's EOD. (B) Raster plot representing the amplitude (abscissa) of field potentials evoked by the EOD in the magnocellularis nucleus (the time course of the experiment concurrent with A). (C) Raster plot representing the amplitude (abscissa) of field potentials evoked by the EOD in the magnocellularis nucleus (the time course of the experiment concurrent with A and B). Below rasters B and C are the corresponding distributions as amplitude histograms. Note the larger dispersion of histogram B compared with histogram C. Reproduced from Nogueira and Caputi (Nogueira and Caputi, 2011).

signals. *Gymnotus omarorum* are solitary animals that show transient accelerations in the presence of a neighboring fish discharging its EO with a similar rate. These behaviors cause an increase of the probability of allo-generated signals directly after the fish's own EODs and a decrease of the probability of the self-generated signals after the conspecific EODs. The spherical neurons block the spikes evoked by the allo-generated events (or add variability to their latency). This task is supported by a K^+_{LT} conductance characteristic of the one-spike-onset neurons. In contrast, self-generated signals are less affected because the pacemaker phase modulation reduces the probability of allo-generated signals before the EOD. In this way, information transmission balance is affected in favor of self-generated signals.

In the presence of the interference, this mechanism facilitates the reception of a steadier stream of self-generated signals at higher centers. This mechanism is an alternative to those shown by pulse mormyriforms and wave-type electric fish for streaming electrosensory signals. Interestingly, pulse species showing a gregarious behavior also lack the long refractory period of homologous spherical neurons (Matsushita et al., 2012), suggesting differences in the sensory hierarchy of active electrolocation and communication signals between both taxa.

One-spike-onset neurons may play several functional roles in sensory systems. This role depends on specific adaptation of the 'response functions' of the neurons and also on the circuit and the functional contexts in which the neuron function is involved. The study of the spherical neurons of the fast electrosensory pathway of *G. omarorum* depicted a still undescribed function of this neuron phenotype, and has opened the question about the existence of a similar signal filtering function in other systems.

References

Aguilera, P. A., Castelló, M. E. and Caputi, A. A. (2001). Electroreception in *Gymnotus carapo*: differences between self-generated and conspecific-generated signal carriers. *J. Exp. Biol.* **204**, 185-198.

Arbib, M., Érdi, P. and Szentagotai, J. (1998). A functional overview. In *Neural Organization: Structure, Function, and Dynamics* (ed. M. A. Arbib), pp. 35-67. Cambridge, MA: MIT Press.

Bacelo, J., Engelmann, J., Hollmann, M., von der Emde, G. and Grant, K. (2008). Functional foveae in an electrosensory system. *J. Comp. Neurol.* **511**, 342-359.

Baker, C. L. (1980). Jamming avoidance behavior in gymnotoid electric fish with pulse-type discharges: sensory encoding for a temporal pattern discrimination. *J. Comp. Physiol. A* **136**, 165-181.

Baker, C. L. (1981). Sensory control of pacemaker acceleration and deceleration in gymnotiform electric fish with pulse-type discharges. *J. Comp. Physiol. A* **141**, 197-206.

Bal, R. and Oertel, D. (2000). Hyperpolarization-activated, mixed-cation current (I_h) in octopus cells of the mammalian cochlear nucleus. *J. Neurophysiol.* **84**, 806-817.

Bal, R. and Oertel, D. (2001). Potassium currents in octopus cells of the mammalian cochlear nucleus. *J. Neurophysiol.* **86**, 2299-2311.

Bastian, J. (1976). Frequency response characteristics of electroreceptors in weakly electric fish (Gymnotidei) with a pulse discharge. *J. Comp. Physiol. A* **112**, 165-180.

Bastian, J. (1986a). Electrolocation: behavior, anatomy and physiology. In *Electroreception* (ed. T. H. Bullock and W. Heiligenberg), pp. 577-612. New York, NY: Wiley.

Bastian, J. (1986b). Gain control in the electrosensory system: a role for the descending projections to the electrosensory lateral line lobe. *J. Comp. Physiol. A* **158**, 505-515.

Bastian, J. (1995). Pyramidal-cell plasticity in weakly electric fish: a mechanism for attenuating responses to reafferent electrosensory inputs. *J. Comp. Physiol. A* **176**, 63-73.

Bastian, J. (1999). Plasticity of feedback inputs in the apteronotid electrosensory system. *J. Exp. Biol.* **202**, 1327-1337.

Bell, C. C. (1981). An efference copy which is modified by reafferent input. *Science* **214**, 450-453.

Bell, C. C. and Grant, K. (1989). Corollary discharge inhibition and preservation of temporal information in a sensory nucleus of mormyrid electric fish. *J. Neurosci.* **9**, 1029-1044.

Bell, C. C. and Maler, L. (2005). Central neuroanatomy of electrosensory systems in fish. In *Electroreception* (T. H. Bullock, C. D. Hopkins, A. N. Popper and R. R. Fay), pp. 68-111. New York, NY: Springer Science and Business Media.

Bell, C. C., Caputi, A. A., Grant, K. and Serrier, J. (1993). Storage of a sensory pattern by anti-Hebbian synaptic plasticity in an electric fish. *Proc. Natl. Acad. Sci. USA* **90**, 4650-4654.

Bell, C. C., Dunn, K., Hall, C. and Caputi, A. A. (1995). Electric organ corollary discharge pathways in mormyrid fish: I. The mesencephalic command associated nucleus. *J. Comp. Physiol. A* **177**, 449-462.

Bell, C. C., Caputi, A. A. and Grant, K. (1997a). Physiology and plasticity of morphologically identified cells in the mormyrid electrosensory lobe. *J. Neurosci.* **17**, 6409-6423.

Bell, C. C., Han, V. Z., Sugawara, Y. and Grant, K. (1997b). Synaptic plasticity in a cerebellum-like structure depends on temporal order. *Nature* **387**, 278-281.

Bennett, M. V. L. (1967). Mechanisms of electroreception. In *Lateral Line Detectors* (ed. P. Cahn), pp. 313-393. Bloomington, IN: Indiana University Press.

Bennett, M. V. L. (1970). Comparative physiology: electric organs. *Annu. Rev. Physiol.* **32**, 471-528.

Bennett, M. V. L. (1971). Electric organs. In *Fish Physiology* (ed. W. S. Hoar and D. J. Randall), pp. 347-491. London: Academic Press.

Berman, N. J. and Maler, L. (1999). Neural architecture of the electrosensory lateral line lobe: adaptations for coincidence detection, a sensory searchlight and frequency-dependent adaptive filtering. *J. Exp. Biol.* **202**, 1243-1253.

Borst, A. and Theunissen, F. E. (1999). Information theory and neural coding. *Nat. Neurosci.* **2**, 947-957.

Brew, H. M. and Forsythe, I. D. (1995). Two voltage-dependent K⁺ conductances with complementary functions in postsynaptic integration at a central auditory synapse. *J. Neurosci.* **15**, 8011-8022.

Bullock, T. H. (1969). Species differences in effect on electroreceptor input on electric organ pacemakers and other aspects of behavior in electric fish. *Brain Behav. Evol.* **2**, 85-101.

Bullock, T. H. and Heiligenberg, W. (1986). *Electroreception.* New York, NY: Wiley.

Bullock, T. H., Hagiwara, S., Kusano, K. and Negishi, K. (1961). Evidence for a category of electroreceptors in the lateral line of gymnotid fishes. *Science* **134**, 1426-1427.

Bullock, T. H., Hamstra, R. H. and Scheich, H. (1972). The jamming avoidance response of high frequency electric fish. *J. Comp. Physiol. A* **77**, 1-22.

Bullock, T. H., Beherend, K. and Heiligenberg, W. (1975). Comparison of the jamming avoidance responses in gymnotoid and gymnarchid electric fish: a case of convergent evolution of behavior and its sensory basis. *J. Comp. Physiol. A* **103**, 97-121.

Bullock, T. H., Hopkins, C. D., Popper, A. N. and Fay, R. R. (2005). *Electroreception.* New York, NY: Springer.

Capurro, A., Macadar, O., Perrone, R. and Pakdaman, K. (1998). Computational model of the jamming avoidance response in the electric fish *Gymnotus carapo. Biosystems* **48**, 21-27.

Capurro, A., Pakdaman, K., Perrone, R. and Macadar, O. (1999). Analysis of the jamming avoidance response in the electric fish *Gymnotus carapo. Biol. Cybern.* **80**, 269-283.

Caputi, A. A. (2012). Timing self-generated actions for sensory streaming. In *Lecture Notes in Computer Science*, Vol. 7552 (ed. A. E. P. Villa, W. Duch, P. Érdi, F. Masulli and G. Palm), pp. 217-222. Berlin: Springer.

Caputi, A. A. and Budelli, R. (1995). The electric image in weakly electric fish: I. A data-based model of waveform generation in *Gymnotus carapo. J. Comput. Neurosci.* **2**, 131-147.

Caputi, A. A. and Nogueira, J. (2012). Identifying self- and nonself-generated signals: lessons from electrosensory systems. *Adv. Exp. Med. Biol.* **739**, 107-125.

Caputi, A. A., Aguilera, P. A. and Castelló, M. E. (2003). Probability and amplitude of novelty responses as a function of the change in contrast of the reafferent image in *G. carapo. J. Exp. Biol.* **206**, 999-1010.

Caputi, A. A., Castelló, M. E., Aguilera, P. A., Pereira, C., Nogueira, J., Rodríguez-Cattáneo, A. and Lezcano, C. (2008). Active electroreception in *Gymnotus omari*: imaging, object discrimination, and early processing of actively generated signals. *J. Physiol. Paris* **102**, 256-271.

Caputi, A. A., Aguilera, P. A. and Pereira, A. C. (2011). Active electric imaging: body-object interplay and object's 'electric texture'. *PLoS ONE* **6**, e22793.

Carlson, B. A. (2009). Temporal-pattern recognition by single neurons in a sensory pathway devoted to social communication behavior. *J. Neurosci.* **29**, 9417-9428.

Carlson, B. A. and Hopkins, C. D. (2004). Stereotyped temporal patterns in electrical communication. *Anim. Behav.* **68**, 867-878.

Carr, C. E. (1993). Processing of temporal information in the brain. *Annu. Rev. Neurosci.* **16**, 223-243.

Carr, C. and Maler, L. (1986). Electroreception in gymnotiform fish. Central anatomy and physiology. In *Electroreception* (ed. T. H. Bullock and W. Heiligenberg), pp. 319-373. New York, NY: Wiley.

Carr, C. E., Heiligenberg, W. and Rose, G. J. (1986a). A time-comparison circuit in the electric fish midbrain. I. Behavior and physiology. *J. Neurosci.* **6**, 107-119.

Carr, C. E., Maler, L. and Taylor, B. (1986b). A time-comparison circuit in the electric fish midbrain. II. Functional morphology. *J. Neurosci.* **6**, 1372-1383.

Carr, C. E., Soares, D., Parameshwaran, S. and Perney, T. (2001). Evolution and development of time coding systems. *Curr. Opin. Neurobiol.* **11**, 727-733.

Carr, C. E., Iyer, S., Soares, D., Kalluri, S. and Simon, J. Z. (2005). Are neurons adapted for specific computations? Examples from temporal coding in the auditory system. In *23 Problems in Systems Neuroscience* (ed. J. L. van Hemmen and T. J. Sejnowski), pp. 245-265. New York, NY: Oxford University Press.

Castelló, M. E., Caputi, A. A. and Trujillo-Cenóz, O. (1998). Structural and functional aspects of the fast electrosensory pathway in the electrosensory lateral line lobe of the pulse fish *Gymnotus carapo. J. Comp. Neurol.* **401**, 549-563.

Castelló, M. E., Aguilera, P. A., Trujillo-Cenóz, O. and Caputi, A. A. (2000). Electroreception in *Gymnotus carapo*: pre-receptor processing and the distribution of electroreceptor types. *J. Exp. Biol.* **203**, 3279-3287.

Catania, K. C. and Kaas, J. H. (1997). Somatosensory fovea in the star-nosed mole: behavioral use of the star in relation to innervation patterns and cortical representation. *J. Comp. Neurol.* **387**, 215-233.

Catania, K. C., Collins, C. E. and Kaas, J. H. (2000). Organization of sensory cortex in the East African hedgehog (*Atelerix albiventris*). *J. Comp. Neurol.* **421**, 256-274.

Chialvo, D. R. (2003). How we hear what is not there: a neural mechanism for the missing fundamental illusion. *Chaos* **13**, 1226-1230.

Churchland, P., Koch, C. and Sejnowski, T. (1990). What is computational neuroscience? In *Computational Neuroscience* (ed. E. L. Schwartz). Cambridge, MA: MIT Press.

Coates, C. W., Altamirano, M. and Grundfest, H. (1954). Activity in electrogenic organs of knife fishes. *Science* **120**, 845-846.

Comas, V. and Borde, M. (2010). Neural substrate of an increase in sensory sampling triggered by a motor command in a gymnotid fish. *J. Neurophysiol.* **104**, 2147-2157.

Crapse, T. B. and Sommer, M. A. (2008). Corollary discharge across the animal kingdom. *Nat. Rev. Neurosci.* **9**, 587-600.

Curti, S., Falconi, A., Morales, F. R. and Borde, M. (1999). Mauthner cell-initiated electromotor behavior is mediated via NMDA and metabotropic glutamatergic receptors on medullary pacemaker neurons in a gymnotid fish. *J. Neurosci.* **19**, 9133-9140.

Curti, S., Comas, V., Rivero, C. and Borde, M. (2006). Analysis of behavior-related excitatory inputs to a central pacemaker nucleus in a weakly electric fish. *Neuroscience* **140**, 491-504.

Dye, J. (1987). Dynamics and stimulus-dependence of pacemaker control during behavioral modulations in the weakly electric fish, *Apteronotus. J. Comp. Physiol. A* **161**, 175-185.

Dye, J. and Heiligenberg, W. (1987). Intracellular recording in the medullary pacemaker nucleus of the weakly electric fish, *Apteronotus*, during modulatory behaviors. *J. Comp. Physiol. A* **161**, 187-200.

Dye, J. C. and Meyer, J. H. (1986). Central control of the electric organ discharge in weakly electric fish. In *Electroreception* (ed. T. H. Bullock and W. Heiligenberg), pp. 71-102. New York, NY: John Wiley.

Engler, G. and Zupanc, G. K. (2001). Differential production of chirping behavior evoked by electrical stimulation of the weakly electric fish, *Apteronotus leptorhynchus. J. Comp. Physiol. A* **187**, 747-756.

Fessard, A. (1974). *Electroreceptors and Other Specialized Receptors in Lower Vertebrates Series: Handbook of Sensory Physiology,* Vol. 3. New York, NY: Springer-Verlag.

Golding, N. L., Robertson, D. and Oertel, D. (1995). Recordings from slices indicate that octopus cells of the cochlear nucleus detect coincident firing of auditory nerve fibers with temporal precision. *J. Neurosci.* **15**, 3138-3153.

Golding, N. L., Ferragamo, M. J. and Oertel, D. (1999). Role of intrinsic conductances underlying responses to transients in octopus cells of the cochlear nucleus. *J. Neurosci.* **19**, 2897-2905.

Grant, K., Bell, C. C., Clausse, S. and Ravaille, M. (1986). Morphology and physiology of the brainstem nuclei controlling the electric organ discharge in mormyrid fish. *J. Comp. Neurol.* **245**, 514-530.

Grant, K., von der Emde, G., Sena, L. G. and Mohr, C. (1999). Neural command of electromotor output in mormyrids. *J. Exp. Biol.* **202**, 1399-1407.

Grau, H. J. and Bastian, J. (1986). Neural correlates of novelty detection in pulse-type weakly electric fish. *J. Comp. Physiol. A* **159**, 191-200.

Heiligenberg, W. (1977). *Principles of Electrolocation and Jamming Avoidance in Electric Fish. Studies of Brain Function*, Vol. 1. Berlin: Springer-Verlag.

Heiligenberg, W. (1991). *Neural Nets in Electric Fish.* Cambridge, MA: MIT Press.

Heiligenberg, W. and Rose, G. (1985). Phase and amplitude computations in the midbrain of an electric fish: intracellular studies of neurons participating in the jamming avoidance response of *Eigenmannia. J. Neurosci.* **5**, 515-531.

Heiligenberg, W. and Rose, G. (1986). Gating of sensory information: joint computations of phase and amplitude data in the midbrain of the electric fish, *Eigenmannia. J. Comp. Physiol. A* **159**, 311-324.

Heiligenberg, W., Baker, C. and Bastian, J. (1978). The jamming avoidance response in gymnotoid pulse-species: a mechanism to minimize the probability of pulse-train coincidence. *J. Comp. Physiol. A* **124**, 211-224.

Hopkins, C. D. (1974a). Electric communication in fish. *Am. Sci.* **62**, 426-437.

Hopkins, C. D. (1974b). Electric communication in the reproductive behavior of *Sternopygus macrurus* (Gymnotoidei). *Z. Tierpsychol.* **35**, 518-535.

Hopkins, C. D. (1976). Stimulus filtering and electroreception: tuberous electroreceptors in three species of gymnotoid fish. *J. Comp. Physiol.* **111**, 171-207.

Hopkins, C. D. (1999). Design features for electric communication. *J. Exp. Biol.* **202**, 1217-1228.

Izhikevich, E. M. (2006). *Dynamical Systems in Neuroscience: The Geometry of Excitability and Bursting* (ed. T. J. Sejnowski and T. A. Poggio), pp. 8-18. Cambridge, MA: MIT press.

Jain, N., Catania, K. C. and Kaas, J. H. (1998). A histologically visible representation of the fingers and palm in primate area 3b and its immutability following long-term deafferentations. *Cereb. Cortex* **8**, 227-236.

Jun, J. J., Harvey-Girard, E., Longtin A. and Maler, L. (2012). Spatial memory shapes active sensory sampling in pulse-type electric fish. *Front. Behav. Neurosci. Conference Abstract: Tenth International Congress of Neuroethology.* doi: 10.3389/conf.fnbeh.2012.27.00087.

Jusczyk, P. W. (1999). How infants begin to extract words from speech. *Trends Cogn. Sci.* **3**, 323-328.

Kalmijn, A. J. (1974)**.** The detection of electric fields from inanimate and animate sources other than electric organs. In: *Handbook of Sensory Physiology*, Vol. 3 (ed. A. Fessard), pp. 147-200. Berlin: Springer-Verlag.

Kawasaki, M. (1996). Comparative analysis of the jamming avoidance response in African and South American wave-type electric fishes. *Biol. Bull.* **191**, 103-108.

Kawasaki, M. (2005). Physiology of tuberous electrosensory systems. In *Electroreception* (ed. T. H. Bullock, C. D. Hopkins, A. N. Popper and R. R. Fay), pp. 154-194. New York, NY: Springer.

Kawasaki, M. and Heiligenberg, W. (1988). Individual prepacemaker neurons can modulate the pacemaker cycle of the gymnotiform electric fish, *Eigenmannia. J. Comp. Physiol. A* **162**, 13-21.

Kawasaki, M., Maler, L., Rose, G. J. and Heiligenberg, W. (1988). Anatomical and functional organization of the prepacemaker nucleus in gymnotiform electric fish: the accommodation of two behaviors in one nucleus. *J. Comp. Neurol.* **276**, 113-131.

Keller, C. H. and Heiligenberg, W. (1989). From distributed sensory processing to discrete motor representations in the diencephalon of the electric fish, *Eigenmannia. J. Comp. Physiol. A* **164**, 565-576.

Keller, C. H., Maler, L. and Heiligenberg, W. (1990). Structural and functional organization of a diencephalic sensory-motor interface in the gymnotiform fish, *Eigenmannia. J. Comp. Neurol.* **293**, 347-376.

Koch, U. and Grothe, B. (2003). Hyperpolarization-activated current (I_h) in the inferior colliculus: distribution and contribution to temporal processing. *J. Neurophysiol.* **90**, 3679-3687.

Kramer, B. (1990). *Electrocommunication in Teleost Fishes. Behavior and Experiments* (*Zoophysiology*), Vol. 29. Berlin: Springer.

Lewis, J. E. and Maler, L. (2002). Dynamics of electrosensory feedback: short-term plasticity and inhibition in a parallel fiber pathway. *J. Neurophysiol.* **88**, 1695-1706.

Lissmann, H. W. (1958). On the function and evolution of electric organs in fish. *J. Exp. Biol.* **35**, 156-191.

Lissmann, H. W. and Machin, K. E. (1958). The mechanism of object location in *Gymnarchus niloticus* and similar fish. *J. Exp. Biol.* **35**, 451-486.

Llinás, R. R. (1988). The intrinsic electrophysiological properties of mammalian neurons: insights into central nervous system function. *Science* **242**, 1654-1664.

Llinás, R. (2001). *I of the Vortex: From Neurons to Self.* A Bradford book, pp. 69-92. Cambridge, MA: MIT Press.

Lorente de Nó, R. (1922). La corteza cerebral del ratón (Primera contribución – la corteza acústica). *Trab. Lab. Invest. Biol.* **20**, 41-78.

Lorenzo, D. and Macadar, O. (2005). Influence of temperature and reproductive state upon the jamming avoidance response in the pulse-type electric fish *Brachyhypopomus pinnicaudatus. J. Comp. Physiol. A* **191**, 85-94.

MacLeod, K. M., Soares, D. and Carr, C. E. (2006). Interaural timing difference circuits in the auditory brainstem of the emu (*Dromaius novaehollandiae*). *J. Comp. Neurol.* **495**, 185-201.

Maler, L. (1979). The posterior lateral line lobe of certain gymnotoid fish: quantitative light microscopy. *J. Comp. Neurol.* **183**, 323-363.

Manis, P. B. and Marx, S. O. (1991). Outward currents in isolated ventral cochlear nucleus neurons. *J. Neurosci.* **11**, 2865-2880.

Marder, E. (2011). Variability, compensation, and modulation in neurons and circuits. *Proc. Natl. Acad. Sci. USA* **108 Suppl. 3**, 15542-15548.

Marr, D. (1982). *Vision.* New York, NY: Freeman.

Matsushita, A., Pyon, G. and Kawasaki, M. (2012). Time disparity sensitive behavior and its neural substrates of a pulse-type gymnotiform electric fish, *Brachyhypopomus gauderio. J. Comp. Physiol. A* [Epub ahead of print] doi: 10.1007/s00359-012-0784-4.

Mehaffey, W. H., Fernandez, F. R., Rashid, A. J., Dunn, R. J. and Turner, R. W. (2006). Distribution and function of potassium channels in the electrosensory lateral line lobe of weakly electric apteronotid fish. *J. Comp. Physiol. A* **192**, 637-648.

Migliore, M. and Shepherd, G. M. (2005). Opinion: an integrated approach to classifying neuronal phenotypes. *Nat. Rev. Neurosci.* **6**, 810-818.

Moller, P. (1995). *Electric Fishes: History and Behavior.* London: Chapman and Hall.

Moortgat, K. T., Keller, C. H., Bullock, T. H. and Sejnowski, T. J. (1998). Submicrosecond pacemaker precision is behaviorally modulated: the gymnotiform electromotor pathway. *Proc. Natl. Acad. Sci. USA* **95**, 4684-4689.

Moortgat, K. T., Bullock, T. H. and Sejnowski, T. J. (2000). Precision of the pacemaker nucleus in a weakly electric fish: network versus cellular influences. *J. Neurophysiol.* **83**, 971-983.

Nogueira, J. and Caputi, A. A. (2011). Timing actions to avoid refractoriness: a simple solution for streaming sensory signals. *PLoS ONE* **6**, e22159.

Nogueira, J., Castelló, M. E. and Caputi, A. A. (2006). The role of single spiking spherical neurons in a fast sensory pathway. *J. Exp. Biol.* **209**, 1122-1134.

Oertel, D., Bal, R., Gardner, S. M., Smith, P. H. and Joris, P. X. (2000). Detection of synchrony in the activity of auditory nerve fibers by octopus cells of the mammalian cochlear nucleus. *Proc. Natl. Acad. Sci. USA* **97**, 11773-11779.

Ortega y Gasset, J. (1914). Meditaciones del Quijote. *Madrid: Publ. Residencia Estud.*, **1**, 32.

Parameshwaran, S., Carr, C. E. and Perney, T. M. (2001). Expression of the Kv3.1 potassium channel in the avian auditory brainstem. *J. Neurosci.* **21**, 485-494.

Penfield, W. and Boldrey, E. (1937). Somatic motor and sensory representation in the cerebral cortex of man as studied by electrical stimulation. *Brain* **60**, 389-443.

Pereira, A. C., Centurión, V. and Caputi, A. A. (2005). Contextual effects of small environments on the electric images of objects and their brain evoked responses in weakly electric fish. *J. Exp. Biol.* **208**, 961-972.

Perrone, R., Macadar, O. and Silva, A. (2009). Social electric signals in freely moving dyads of *Brachyhypopomus pinnicaudatus. J. Comp. Physiol. A* **195**, 501-514.

Post, N. and von der Emde, G. (1999). The 'novelty response' in an electric fish: response properties and habituation. *Physiol. Behav.* **68**, 115-128.

Prescott, S. A. and Koninck, Y. D. (2002). Four cell types with distinctive membrane properties and morphologies in lamina I of the spinal dorsal horn of the adult rat. *J. Physiol.* **539**, 817-836.

Quintana, L., Sierra, F., Silva, A. and Macadar, O. (2011). A central pacemaker that underlies the production of seasonal and sexually dimorphic social signals: functional aspects revealed by glutamate stimulation. *J. Comp. Physiol. A* **197**, 211-225.

Ramón y Cajal, S. (1899). *Textura del Sistema Nervioso del Hombre y de los Vertebrados.* Madrid: Imprenta y Librería de Nicolás Moya.

Rathouz, M. and Trussell, L. (1998). Characterization of outward currents in neurons of the avian nucleus magnocellularis. *J. Neurophysiol.* **80**, 2824-2835.

Réthelyi, M. and Szabo, T. (1973). Neurohistological analysis of the lateral lobe in a weakly electric fish, *Gymnotus carapo* (Gymnotidae, Pisces). *Exp. Brain Res.* **18**, 323-339.

Reyes, A. D., Rubel, E. W. and Spain, W. J. (1994). Membrane properties underlying the firing of neurons in the avian cochlear nucleus. *J. Neurosci.* **14**, 5352-5364.

Richer-de-Forges, M. M., Crampton, W. G. R. and Albert, J. S. (2009). A new species of *Gymnotus* (Gymnotiformes, Gymnotidae) from Uruguay: description of a model species in neurophysiological research. *Copeia* **2009**, 538-544.

Rodríguez-Cattáneo, A., Pereira, A. C., Aguilera, P. A., Crampton, W. G. and Caputi, A. A. (2008). Species-specific diversity of a fixed motor pattern: the electric organ discharge of *Gymnotus. PLoS ONE* **3**, e2038.

Rodríguez-Cattáneo, A., Aguilera, P., Cilleruelo, E., Crampton, W. G. R. and Caputi, A. A. (2013). Electric organ discharge diversity in the genus *Gymnotus*: anatomo-functional groups and electrogenic mechanisms. *J. Exp. Biol.* **216**, 1501-1515.

Rose, G. and Heiligenberg, W. (1986). Limits of phase and amplitude sensitivity in the torus semicircularis of *Eigenmannia. J. Comp. Physiol. A* **159**, 813-822.

Scheich, H. and Bullock, T. H. (1974). The detection of electric fields from electric organs. In *Electroreceptors and Other Specialized Receptors in Lower Vertebrates (Handbook of Sensory Physiology)* Vol. 3 (ed. A. Fessard), pp. 201-256. New York, NY: Springer-Verlag.

Schlegel, P. A. (1973). Perception of objects in weakly electric fish *Gymnotus carapo* as studied in recordings from rhombencephalic neurons. *Exp. Brain Res.* **18**, 340-354.

Silva, A., Perrone, R. and Macadar, O. (2007). Environmental, seasonal, and social modulations of basal activity in a weakly electric fish. *Physiol. Behav.* **90**, 525-536.

Soares, D., Chitwood, R. A., Hyson, R. L. and Carr, C. E. (2002). Intrinsic neuronal properties of the chick nucleus angularis. *J. Neurophysiol.* **88**, 152-162.

Sotelo, C., Réthelyi, M. and Szabo, T. (1975). Morphological correlates of electrotonic coupling in the magnocellular mesencephalic nucleus of the weakly electric fish *Gymnotus carapo. J. Neurocytol.* **4**, 587-607.

Sperry, R. W. (1950). Neural basis of the spontaneous optokinetic response produced by visual inversion. *J. Comp. Physiol. Psychol.* **43**, 482-489.

Spiro, J. E. (1997). Differential activation of glutamate receptor subtypes on a single class of cells enables a neural oscillator to produce distinct behaviors. *J. Neurophysiol.* **78**, 835-847.

Szabo, T. (1967). Activity of peripheral and central neurons involved in electroreception. In: *Lateral Line Detectors* (ed. P. Cahn), pp. 295-311. Bloomington, IN: Indiana University Press.

Szabo, T., Sakata, H. and Ravaille, M. (1975). An electrotonically coupled pathway in the central nervous system of some teleost fish, Gymnotidae and Mormyridae. *Brain Res.* **95**, 459-474.

Tartini, G. (1754). *Trattato Di Musica Secondo La Vera Scienza Del' Armonía.* Padova, Italy: Giovanni Manfrè.

Trussell, L. O. (1999). Synaptic mechanisms for coding timing in auditory neurons. *Annu. Rev. Physiol.* **61**, 477-496.

von Holst, E. and Mittelstaedt, H. (1950). Das Reafferenzprincip. *Naturwissenschaften.* **37**, 464-476.

Wagner, H. and Gaese, B. (2005). Can we understand the action of brains in natural enviroments? In *23 Problems in Systems Neuroscience* (ed. J. L. van Hemmen and T. J. Sejnowski), pp. 22-43. New York, NY: Oxford University Press.

Watanabe, A. and Takeda, K. (1963). The change of discharge frequency by A.C. stimulus in a weakly electric fish. *J. Exp. Biol.* **40**, 57-66.

Watson, D. and Bastian, J. (1979). Frequency response characteristics of electroreceptors in the weakly electric fish *Gymnotus carapo. J. Comp. Physiol. A* **134**, 191-202.

Westby, G. W. M. (1974). Assessment of the signal value of certain discharge patterns in the electric fish *Gymnotus carapo* by means of playback. *J. Comp. Physiol. A* **92**, 327-341.

Westby, G. W. M. (1979). Electrical communication and jamming avoidance between resting *Gymnotus carapo. Behav. Ecol. Sociobiol.* **4**, 381-393.

Westby, G. W. M. (1981). Communication and jamming avoidance in electric fish. *Trends Neurosci.* **4**, 205-210.

Wu, S. H. and Oertel, D. (1984). Intracellular injection with horseradish peroxidase of physiologically characterized stellate and bushy cells in slices of mouse anteroventral cochlear nucleus. *J. Neurosci.* **4**, 1577-1588.

Yager, D. D. and Hopkins, C. D. (1993). Directional characteristics of tuberous electroreceptors in the weakly electric fish, *Hypopomus* (Gymnotiformes). *J. Comp. Physiol. A* **173**, 401-414.

Yan, N., Li, X. H., Cheng, Q., Yan, J., Ni, X. and Sun, J. H. (2007). [Decreased A-type potassium current mediates the hyperexcitability of nociceptive neurons in the chronically compressed dorsal root ganglia]. *Sheng Li Xue Bao* **59**, 240-246.